the Courant limitation on the choice of time step for stability. The results for the same test case using a QUICKEST scheme are shown in Fig. 3. Although only one severe test case has been sudied in this short work, the study is being extended to cover a wide range of spatial resolutions and also to include the effects of a diffusion term. Finally, recent work by Manson and Wallis[7] (DISCUS), Roache[8] (FBMMOC), and Leonard et al.[9] (NIRVANA) may suggest ways to achieve unconditionally stable unsteady simulations.

Acknowledgment

The authors wish to thank B. P. Leonard for his helpful comments on an earlier draft of this paper.

References

[1]Freitas, C. J., "Perspective: Selected Benchmarks from Commercial CFD Codes," *Journal of Fluids Engineering*, Vol. 117, June 1995, pp. 208–218.

[2]Patankar, S. V., *Numerical Heat Transfer and Fluid Flow*, Hemisphere, New York, 1980.

[3]Leonard, B. P., "A Stable and Accurate Convective Modeling Procedure Based on Quadratic Upstream Interpolation," *Computer Methods in Applied Mechanics and Engineering*, Vol. 19, No. 1, 1979, pp. 59–98.

[4]Chen, Y., and Falconer, R. A., "Advection-Diffusion Using the Modified QUICK Scheme," *International Journal of Numerical Methods in Fluids*, Vol. 15, No. 10, 1992, pp. 1171–1196.

[5]Gaskell, P. H., and Lau, A. K. C., "Curvature-Compensated Convective Transport: SMART, A New Boundedness-Preserving Transport Algorithm," *International Journal of Numerical Methods in Fluids*, Vol. 8, No. 6, 1988, pp. 617–641.

[6]Wallis, S. G., and Manson, J. R., "Numerical Simulation of Solute Transport Using the QUICKEST Algorithm," *Hydraulic Modelling: Development and Application of Hydraulic Models*, edited by A. J. Saul, Publication No. 11, BHR Group, 1994.

[7]Manson, J. R., and Wallis, S. G., "An Accurate Numerical Algorithm for Advective Transport," *Communications in Numerical Methods in Engineering* (to be published).

[8]Roache, P. J., "A Flux-Based Modified Method of Characteristics," *International Journal of Numerical Methods in Fluids*, Vol. 15, No. 11, 1992, pp. 1259–1275.

[9]Leonard, B. P., Lock, A. P., and MacVean, M. K., "The NIRVANA Scheme Applied to One Dimensional Advection," *International Journal of Numerical Methods for Heat and Fluid Flow*, Vol. 5, No. 4, 1995, pp. 341–377.

Simulating Heat Addition via Mass Addition in Variable Area Compressible Flows

W. H. Heiser,* W. B. McClure,† and C. W. Wood†
U.S. Air Force Academy, Colorado 80840-6222

Introduction

THE authors recently demonstrated the striking and potentially useful similarity between the influence of heat addition and mass addition (injected normal to the flow with the same total temperature and composition) on constant area compressible duct flows.[1] This was primarily accomplished by means of closed-form, mathematical solutions for flows involving a single forcing function (e.g., heat or mass addition), commonly known as simple flows.[2] The analyses were primarily based on the classical one-dimensional model of the steady, frictionless, constant throughflow area flow of a calorically perfect gas.[2] The similarities were also found to exist when wall friction is present, including the estimated point of boundary-layer separation in supersonic flow. This article extends the prior results to incorporate the influence of throughflow area variation.

Received Feb. 1, 1995; accepted for publication Nov. 20, 1995.

*Professor, Department of Aeronautics. Fellow AIAA.

†Associate Professor, Department of Aeronautics. Senior Member AIAA.

Multiple Combined Effects

Versatile though it may be, one-dimensional flow analysis cannot provide closed-form solutions for arbitrary distributions of several independent parameters. This applies in particular to the important case of heat (or mass) addition in a duct of varying throughflow area, for which the distribution of both is crucial to the outcome [i.e., the exit conditions depend on more than the total heat (or mass) addition and throughflow area change]. This case is important because it is the essence of dual-mode ramjet/scramjet combustor operation, where choking during ramjet operation results from the cooperation between the chemical energy release that drives the local Mach number up to 1 (hence the term thermal choking) and the throughflow area increase that continues the acceleration beyond Mach 1.[3,4]

A simple numerical procedure was therefore developed to explore cases and design experiments with arbitrary axial distributions of heat addition, mass addition, wall friction, and/or throughflow area. Although the code permits other variations, all of the following discussions of mass addition refer only to the case of injection normal to the duct axis of a gas with the same total temperature and composition as the inlet flow. The algorithm is based on the one-dimensional unsteady Euler equations, cast in a conservative finite volume form and solved using a first-order flux-vector splitting scheme.[5] The working fluid was modeled as a calorically perfect gas with a fixed ratio of specific heats. The duct wall friction force was included in the control volume momentum balance and was modeled via a local wall friction factor. For cases with the inlet Mach number $M_i > 1$, the exit pressure was set low enough to prevent shock wave formation within the duct. For cases with $M_i < 1$, the exit pressure was iteratively adjusted to be compatible with the inlet conditions. The code was run on a Sun SparcStation with 35 megabytes of memory. Initial conditions in the duct were arbitrarily set based on M_i. A typical run of 100,000 global time steps over 100 equally spaced cells took about 15 min. Residual error, quantified as the average absolute fractional change of the local momenta between successive time steps, was of the order of 10^{-7}.

Please note that the differences in the manner in which the fluxes are calculated for supersonic and subsonic cells result in artificial property discontinuities at the transonic transitions (i.e., the sonic point and shock waves). The impact of these discontinuities can be minimized by using a fine grid in such regions, as was done in this study to achieve derivatives of satisfactory accuracy.

Before moving on to the results of computations, it should be noted that closed-form analytical solutions again made an important contribution by providing three useful benchmarks for the development of the code. First, numerical analyses reproduced all of the results described in Ref. 1. Second, generalized one-dimensional flow analysis furnishes the unique position of the choking or sonic point should it occur, as well as the corresponding Mach number axial gradients, even for combined effects, through the well-known "special conditions at the sonic point."[2,3] The algebraic results of this analysis for the typical contemporary dual-mode combustor case of parabolic heat (or mass) addition and linear area distribution are compiled in Table 1, where T_t is the total temperature; $\dot{m}$ is the mass flow; α, τ, and μ are constants of area variation, heat, and mass addition, respectively; A is the local throughflow area; L is the axial length of the duct; M is the local Mach number; γ is the ratio of specific heats; ξ is the dimensionless axial coordinate x/L; the subscript i designates the inlet conditions; and the subscript c indicates the choking or sonic point. The numerical analyses reproduced these results whenever the flow choked. Third, inspection of the complete one-dimensional compressible flow differential equations of Ref. 2 reveals that adding either heat or mass alone should produce identical Mach number, static pressure, and total pressure axial distributions for specified inlet conditions and duct geometry provided only that

$$\frac{d\dot{m}}{\dot{m}} = \frac{1}{2}\frac{dT_t}{T_t} \qquad \text{or} \qquad \frac{\dot{m}}{\dot{m}_i} = \sqrt{\frac{T_t}{T_{ti}}} \tag{1}$$

The axial distributions of other flow properties, such as density, velocity, and static temperature, are not identical but can easily be found from the Mach number axial distribution and the "useful integral relations" of Ref. 2. The numerical analyses of the axial

Table 1 Dimensionless axial position of the sonic point and Mach number axial derivatives at the sonic point for parabolic heat or mass addition and the linear area distribution $A/A_i = 1 + \alpha\xi$

	Heat addition	Mass addition
Choking quantity	$(T_t/T_{ti}) = 1 + \tau[1 - (\xi/2)]\xi$	$(\dot{m}/\dot{m}_i) = 1 + \mu[1 - (\xi/2)]\xi$
ξ_c	$\dfrac{\dfrac{\gamma-1}{2} - \dfrac{\gamma+1}{2\alpha} + \sqrt{\left(\dfrac{\gamma+1}{2\alpha} - \dfrac{\gamma-1}{2}\right)^2 + 2\gamma\left(\dfrac{\gamma+1}{2\alpha} - \dfrac{1}{\tau}\right)}}{\gamma}$	$\dfrac{\gamma - \dfrac{\gamma+1}{\alpha} + \sqrt{\left(\gamma - \dfrac{\gamma+1}{\alpha}\right)^2 + 2(2\gamma+1)\left(\dfrac{\gamma+1}{\alpha} - \dfrac{1}{\mu}\right)}}{2\gamma+1}$
$\left(\dfrac{dM}{d\xi}\right)_c$	$-\dfrac{\Phi_c L}{4} \pm \sqrt{\left(\dfrac{\Phi_c L}{4}\right)^2 - \dfrac{\Psi_c L^2}{4}}$	
$\Phi_c L$	$\dfrac{1}{2}\left\{\dfrac{\gamma(\gamma+1)(1-\xi_c)}{(1/\tau) + [1 - (\xi_c/2)]\xi_c}\right\}$	$\dfrac{\gamma(\gamma+1)(1-\xi_c)}{(1/\mu) + [1 - (\xi_c/2)]\xi_c}$
$\Psi_c L^2$	$\dfrac{\gamma+1}{[(1/\alpha)+\xi_c]^2} - \dfrac{(\gamma+1)^2\left\{(1/\tau) + [1-(\xi_c/2)]\xi_c + (1-\xi_c)^2\right\}}{2\{(1/\tau) + [1-(\xi_c/2)]\xi_c\}^2}$	$\dfrac{\gamma+1}{[(1/\alpha)+\xi_c]^2} - \dfrac{(\gamma+1)^2\left\{(1/\mu) + [1-(\xi_c/2)]\xi_c + (1-\xi_c)^2\right\}}{\{(1/\mu) + [1-(\xi_c/2)]\xi_c\}^2}$

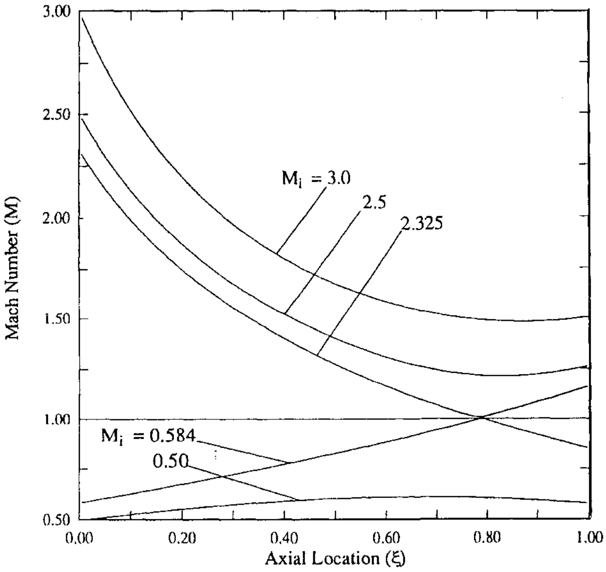

Fig. 1 Results of numerical computations for the variation of axial Mach number with dimensionless axial position for the case of combined mass addition and area variation of Table 1: γ = 1.35, α = 0.25, and μ = 0.50.

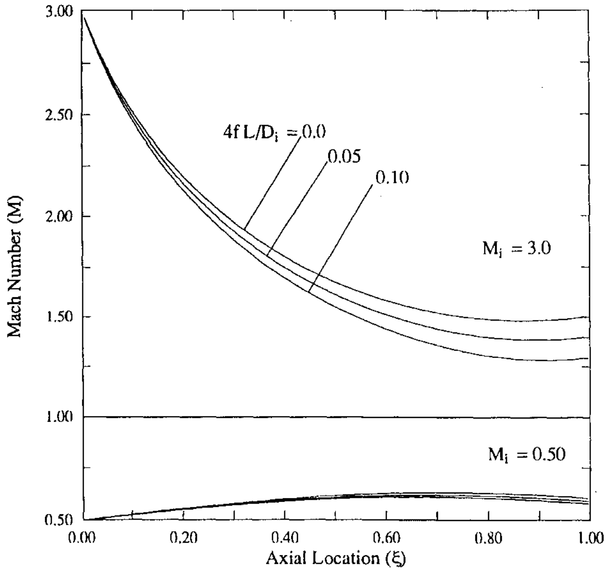

Fig. 2 Results of numerical computations for the case of combined mass addition, area variation, and wall friction: γ = 1.35, α = 0.25, and μ = 0.50. The case of zero wall friction also appears in Fig. 1.

distributions of Mach number, static pressure, and total pressure caused by either heat or mass addition subject to the condition of Eq. (1) could not be distinguished from one another.

Numerical Results

Figure 1 shows the numerically determined axial distribution of Mach number for the case of combined mass addition and throughflow area variation of Table 1 with $\gamma = 1.35$, $\alpha = 0.25$, and $\mu = 0.50$. These results clearly exhibit the classical saddle-point behavior of convergent-divergent nozzles despite the fact that the duct is only divergent. For inlet Mach numbers less than 0.584, provided the exit static pressure is compatible, the flow is everywhere subsonic, and the maximum Mach number occurs within the duct. For inlet Mach numbers greater than 2.325, provided the exit static pressure is set sufficiently low, the flow is everywhere supersonic, and the minimum Mach number occurs within the duct. For a subsonic inlet Mach number of 0.584 and a sufficiently low exit static pressure, the flow chokes within a fraction of a percent of the dimensionless axial location $\xi = 0.780$ given by the equations of Table 1 and is supersonic afterwards. For a supersonic inlet Mach number of 2.325 the flow becomes sonic at the same location. No shock-free solution exists between $0.584 < M_i < 2.325$. The Mach number axial derivatives at the choking or sonic point are within a fraction of a percent of the values +0.670 and −0.811 given by the equations of Table 1.

Finally, Fig. 2 presents results for combined mass addition, throughflow area variation, and wall friction. They correspond to several of the previous cases altered by selecting local skin-friction coefficients of $0 < f < 0.005$ and $L/D_i = 5$ to achieve $0 < 4fL/D_i < 0.10$, where D_i is the inlet hydraulic diameter of the duct.[1,2] Reviewing this information leads to the encouraging conclusion that the presence of ordinary amounts of wall friction should not obscure the dual-mode operation phenomena of interest.

Conclusions

This study extends the examination of the similarity between the influence of heat addition and mass addition on compressible duct flows of Ref. 1. It has provided some new and interesting analytical results and a reliable computer code useful for evaluating the influence of combined effects. The results continue to encourage the belief that relatively modest laboratory experiments employing mass addition can be devised that will reproduce the leading phenomena of heat addition in ducts and particularly of the behavior of dual-mode ramjet/scramjet combustors.

Acknowledgments

We are indebted to the U.S. Air Force Frank J. Seiler Research Laboratory for financial support and the Department of Aeronautics of the U.S. Air Force Academy for its traditional hospitality and operational support of our work. The central concept for this research grew out of stimulating telephone discussions with Edward

T. Curran, now director of the Aero Propulsion and Power Directorate of the Wright Laboratory, that took place in 1992. His continuing interest in the project since then has also been of great value.

References

[1]Heiser, W. H., McClure, W. B., and Wood, C. W., "Simulating Heat Addition via Mass Addition in Constant Area Compressible Flows," *AIAA Journal*, Vol. 33, No. 1, 1995, pp. 167–171.

[2]Shapiro, A. H., *The Dynamics and Thermodynamics of Compressible Fluid Flow*, Ronald, New York, 1953, Chap. 8.

[3]Heiser, W. H., and Pratt, D. T., *Hypersonic Airbreathing Propulsion*, AIAA Education Series, AIAA, Washington, DC, 1994, Chap. 6.

[4]Pratt, D. T., and Heiser, W. H., "Isolator-Combustor Interaction in a Dual-Mode Scramjet Engine," AIAA Paper 93-0358, Jan. 1993.

[5]Van Leer, B., "Flux-Vector Splitting for the Euler Equations," *Lecture Notes in Physics*, Vol. 170, Springer–Verlag, New York, 1982, pp. 507–512.

Dusty Shock Flow with Unstructured Adaptive Finite Elements and Parcels

S. Sivier* and E. Loth†
University of Illinois at Urbana–Champaign, Urbana, Illinois 61801
J. Baum‡
Science Applications International Corporation, McLean, Virginia 22102
and
R. Löhner§
George Mason University, Fairfax, Virginia 22030

I. Introduction

WHEN solving the compressible two-phase equations, the gas as a continuum is best represented by an Eulerian description, i.e., the gas characteristics are calculated at fixed points within the flow. The particles (or droplets), however, may be modeled by either an Eulerian description (in the same manner as the gas flow), or a Lagrangian description (where individual particle groups are monitored and tracked in the flow). Herein, the former will be referred to as an Eulerian–Eulerian (E–E) treatment, whereas the latter will be defined as an Eulerian–Lagrangian (E–L) treatment. Recently, Sivier et al.[1] developed an E–E method using an unstructured grid finite element method–flux corrected transport (FEM–FCT) flow solver in order to examine shock wave attenuation in dusty shock flows. FEM–FCT was designed to be able to capture flow features with large gradients, such as those that occur in density near shocks. Whereas a Lagrangian approach offers many potential advantages, this method also creates potential problems that should be addressed by the model. For instance, large numbers of particles may cause a Lagrangian analysis to be memory intensive (this may be partially offset by using parcels, each of which represents a number of particles in the flow). In addition, continuous mapping and remapping of particles to their respective elements may increase computational requirements, particularly for unstructured grids.

Both E–E and E–L descriptions have been used widely on structured grids,[2,3] but this research seeks a comparative study between these two approaches when coupled with a dynamically adaptive unstructured finite element method with a novel parcel adaptive technique. The objective of the present study was to formulate and develop an E–L method with an adaptive grid FEM–FCT flow solver that is computationally efficient. This method was used to predict a particle laden shock wave attenuation as a test case and to compare performance characteristics (computation speed, memory, and accuracy) with an E–E implementation[1] that also includes adaptive unstructured grids.

Received July 20, 1994; revision received June 27, 1995; accepted for publication June 28, 1995.

*Graduate Research Assistant, Department of Aeronautical and Astronautical Engineering. Student Member AIAA.

†Associate Professor, Department of Aeronautical and Astronautical Engineering. Senior Member AIAA.

‡Senior Research Scientist. Associate Fellow AIAA.

§Research Professor, CSI. Member AIAA.

II. Numerical Method

One particular two-phase flow that includes two-way coupling of interphase momentum transport and compressible flow effects is dusty shock attenuation, which is typically modeled with E–E formulations.[1,4,5] In such a flow, the particle densities are typically two to three orders of magnitude higher than that of the carrier gas, such that particle mass loadings of order unity yield significant modification of the gas flow behavior but with corresponding negligible volume loadings (e.g., less than 1%), such that particle–particle interactions and volume displacement effects can be typically eliminated. We will herein restrict ourselves to such flow conditions. The gas equations used in the current study are the Euler equations with non-homogenous source terms added to represent the interphase momentum and energy transfer.[1,4,5]

Dynamic unstructured grid adaption was employed to optimize the distribution of nodal points by continually refining areas with high gradients of gas density and coarsening areas of low gradients of gas density, where the maximum level of refinement (LOR) is preset. Since we are interested in computing dilute particle flows of negligible volume fraction (but significant mass fraction) with particle diameters on the order of several microns, the present technique assumes particle effects on gas pressures and particle–particle interactions are negligible, and particles are spherical and inert. In addition, since the flow is nonreacting and the particles are relatively small, radiation and gravitational effects are neglected.

The Lagrangian particle description was implemented by tracking individual groups of particles, referred to as parcels.[6,7] The previous timestep's gas characteristics for a host element (the element that contains a given parcel) are linearly interpolated to each parcel coordinate to determine the momentum and energy interphase coupling terms D_i and Q as follows[5]:

$$D_i = \frac{\pi}{8}\frac{\phi_k N_p}{A_e}\rho C_D |u_i - u_{pi}|(u_i - u_{pi})d^2$$

$$Q = \pi d^2 \frac{\phi_k N_p}{A_e}\frac{Nu \cdot k}{d}(T - T_p)$$

where the shape function for parcel p associated with the node k is ϕ_k, the number of particles in parcel p is N_p, the area of the host element is A_e, the Nusselt number is Nu and the thermal conductivity of the gas is k, where u, T, d, u_p, and T_p are the gas velocity and temperature, the particle diameter, velocity, and temperature, respectively, and the subscript i indicates the direction of the velocity in a Cartesian coordinate system and where a conventional C_D formulation given by Clift et al.[8] (as opposed to an unsteady formulation) was shown to yield robust predictive performance for dusty shock attenuation.[1] The parcel shape functions are then used to scatter each parcel's contributions to the host element's nodes; thus, parcel coupling terms within the elements connected to any node are summed in a linear weighting fashion to that node. Further details on the formulation can be found in Sivier et al.[9] The Lagrangian parcel equations[7,10] are then solved with an explicit single-step finite difference formulation for each parcel to update the parcel unknowns. The Lagrangian description involved continuously determining the host element once a parcel had moved or when the unstructured mesh was refined/coarsened. The use of a vectorized successive neighbor search[11] was found to provide an elegant and efficient solution to this problem.

A novel technique was used to make the parcels adapt to the dynamic element distribution by sensing the local parcel population. To locally determine if a refinement or a coarsening of parcels is to be performed, the number of parcels in each element is noted following each mesh refinement. If there are fewer than some preset